Published in final edited form as:
Biochemistry. 2013 April 9; 52(14): 2472–2481. doi:10.1021/bi301625a.

PROTON BRIDGING IN THE INTERACTIONS OF THROMBIN WITH HIRUDIN AND ITS MIMICS[†]

Ildiko M. Kovach[*,‡], **Lazaros Kakalis**[§], **Frank Jordan**[§], and **Daoning Zhang**[//]

[‡]The Catholic University of America, Department of Chemistry, Washington DC 20064

[§]Department of Chemistry at Rutgers, The State University of New Jersey, Newark, New Jersey 07102-1811

[//]Center for Biomolecular Structure & Organization, Department of Chemistry & Biochemistry, University of Maryland, College Park 20742-3360

Abstract

Thrombin is the pivotal serine protease enzyme in the blood cascade system and thus a target of drug design for control of its activity. The most efficient non-physiologic inhibitor of thrombin is hirudin, a naturally occurring small protein. Hirudin and its synthetic mimics employ a range of hydrogen bonding, salt bridging and hydrophobic interactions with thrombin to achieve tight binding with K_i values in the nano- to femtomolar range. The one-dimensional ^{1}H NMR spectrum carried out at 600 MHz reveals a resonance at 15.33 ppm downfield from silanes in complexes between human α-thrombin and r-hirudin in pH 5.6-8.8 buffers and between 5 and 35 °C. There is also a resonance between 15.17 and 15.54 ppm seen in human α-thrombin complexes with hirunorm IV, hirunorm V, an Nα(Me)Arg-peptide, RGD-hirudin and Nα-2-naphthylsulfonyl-glycyl-DL-4-amidinophenylalanyl-piperidide acetate salt (NAPAP), while there is no such low-field resonance observed in a complex of porcine trypsin and NAPAP. The chemical shifts suggest that these resonances represent H-bonded environments. H-donor acceptor distances in the corresponding H-bonds are estimated to be <2.7 Å. Addition of Phe-Pro-Arg-Chloromethylketone (PPACK) to a complex of human α-thrombin with r-hirudin results in an additional signal at 18.03 ppm, which is 0.10 ppm upfield from one observed (Kovach, I. M. *et al. Biochemistry* 2009, *48*, 7296–7304) for thrombin covalently modified with PPACK. In contrast, the peak at 15.33 ppm remains unchanged. The fractionation factors for the thrombin-hirudin type complexes are near 1.0 within 20% error. The most likely site of the short H-bond in thrombin complexes with the hirudin family of inhibitors is in the hydrophobic patch of the C-terminus of hirudin where Glu$^{57'}$ and Glu$^{58'}$ are embedded and interact with Arg^{75} and Arg^{77} and their solvate water (on thrombin). Glu$^{57'}$ and Glu$^{58'}$ present in the hirudin family of inhibitors is a key binding epitope of fibrinogen, thrombin's prime substrate, which lends substantial interest to the SHB as a binding element at the fibrinogen recognition site.

Keywords

Enzyme inhibition mechanisms; blood cascade enzymes; short strong hydrogen bonds; ^{1}H NMR in protein binding

[†]This work was supported in part by the US National Institutes of Health, Grant No 1 R15 HL067754-02.

[*]Corresponding author: Ildiko M. Kovach, The Catholic University of America, Department of Chemistry, Washington DC 20064. Telephone: 202-319-6550; FAX: 202-3195381, kovach@cua.edu.

A key serine protease enzyme in blood clotting is α-thrombin.(1-8) Thrombin catalyzes the hydrolysis of one to four peptide bonds in over a dozen large protein precursors operating in the blood cascade system.(6;7;9-14) Thrombin fulfills two strictly coordinated roles: procoagulant and anticoagulant. Five cofactors participate in substrate binding and the inter-conversion between the two catalytic states referred to as “fast” and “slow”.(7;8;15-17) Cofactors bind to external sites distant from the active site of thrombin to exert a subtle allosteric effect implemented by a slight conformational change. As maintenance of the hemostatic balance has broad implications in human health, the regulation of human α-thrombin with a broad range of inhibitors has been a main target of investigations and drug design.(18-21)

Our interest in the regulation of thrombin function has been in the physicochemical interactions underlying the inhibitory power of certain thrombin effectors. Previously, we examined H-bonding interactions in the covalent adduct between human α-thrombin and PPACK mimicking the oxyanionic tetrahedral intermediate in the acylation step and phosphate and phosphonate ester adducts of thrombin resembling the anionic tetrahedral intermediate in the deacylation step in substrate hydrolysis, using kinetics and high-resolution, low-field ^{1}H NMR signals.(22) Both types of tetra-covalent adducts of thrombin, as many transition-state analog adducts of enzymes with inhibitors, yield a unique resonance in high-resolution ^{1}H NMR spectra between 14 and 21 ppm downfield from silanes.(23-38) These low-field resonances have also been observed at pH below 6 with some native enzymes that catalyze proton transfer.(23;24;34;36-38) The deshielding phenomenon had been attributed to the presence of a short-strong-H-bond (SSHB) at the active site of the enzyme upon protonation of a key base catalyst (His), which occurs even at pH above 6 when the enzyme interacts with a covalent modifier. It has since been shown that the H-bond is most likely one formed between His^{57}δNH and Asp^{102}γO in serine proteases.(22;25-33;35;36;39) The stabilization of SSHBs has been attributed to electrostatic effects, charge, polarization and resonance. Whereas, H-bond donor and acceptor distances associated with the low-field resonances are typically between 2.4 and 2.7 Å and donor-H-acceptor angles > 150°, the unusual strength of the H-bonds claimed earlier has (40) rarely been substantiated.(41-47) In recognition of this circumstance, the short H-bond (SHB) notation is used in this paper.

The proposal that the H-bond donor-acceptor distances across the catalytic triad contract during catalysis originates from the interpretation of solvent deuterium isotope effects on protease-catalyzed reactions.(48-56) The contraction of distances most likely lowers the activation barrier for the nucleophilic attack on carbonyl at the reaction center in serine protease catalysis, as a quantum chemical calculation for RNase A catalysis shows.(40) As thrombin is a very efficient catalyst of the breakdown of its natural and analytical substrates, it also undergoes similar structural changes to stabilize the transition states for hydrolysis of its substrates. This notion is supported by solvent deuterium isotope effects observed between 2.5 and 3.5 in the hydrolysis of many thrombin substrates.(51;52)

We have recently posed a new question: whether or not SHBs exist in tight-binding interactions between enzymes and their cognate (large) substrates. If yes, tight-binding substrate analog inhibitors may exhibit a signal in low-field ^{1}H NMR at high resolution. The hirudin family of inhibitors mimic the binding propensity of fibrinogen to thrombin. Among inhibitors, hirudin presents the greatest affinity for thrombin with a K_i = 20 fM.(7) Hirudin binds to thrombin in a parallel and nonsubstrate mode which sets it apart from many peptide inhibitors. There are at least thirteen intermolecular H-bridges in the x-ray structure of the α-thrombin-r-hirudin (variant 2, Lys^{47}) complex (2.3 Å resolution) interspersed with salt bridges and hydrophobic interactions.(57-59) Most of these interactions occur at the fibrinogen recognition site (FRS or exosite I) of α-thrombin. The FRS is a critical site for

the allosteric regulation of α-thrombin catalysis and inhibition. The C-terminal section of hirudin is more ordered in the complex(57-59) than in the solution (2D) ^{1}H NMR structure of r-hirudin alone,(60-63) when bound to the FRS of α-thrombin. In addition to the intermolecular H-bonds formed in the complex, intramolecular H-bonds near the N-terminus of r-hirudin shorten and numerous short H-bonds form with water.(58) Hirudin mimics, (64-66) which have most key binding elements of hirudin incorporated, became available in recent years. Comparative studies of thrombin complexes with hirudin mimics can guide in elucidating the location of SHBs and enhance the understanding of the specific environment of the SHBs.

Herein, we report the observation and characterization of SHBs that human α-thrombin forms with the noncanonical r-hirudin, its mimics and canonical (binding as antiparallel β sheets) peptide inhibitors. The deuterium isotope effect on the SHBs and their robustness tested in pH dependence, Na^{+} ion dependence and temperature studies of the line width of the resonance are also discussed.

Materials and Methods

Materials

All buffer salts were reagent grade and were purchased from either Aldrich, Fisher, or Sigma Chemical Co. Anhydrous DMSO, heavy water with 99.9 % deuterium content and anhydrous methanol were purchased from Aldrich Chemical Co. The proton sponge 1,8-bis(dimethylamino) naphthalene, MUGB and NAPAP in >93% purity (Fluka), porcine trypsin, Type IX, 24,000 Da, > 15,000 BTA u/mg, 98 % protein and r-hirudin type 2, lyophilized product, >95% pure were from Sigma Chemical Co. r-Hirudin type 1, lyophilized product, >95% pure was from Centerchem Inc. H-D-Phe-Pip-Arg-4-nitroanilide.HCl (S-2238) 99% (TLC) was purchased from Diapharma Group Inc. The inhibitor PPACK was purchased from BioMol Co. Human α-thrombin, 36,500 Da, was purchased either from Enzyme Research Laboratories Inc in 3010 NIH u/mg activity in pH 6.5, 0.05 M sodium citrate buffer, 0.2 M NaCl and 0.1% PEG-8000 or from Haematologic Technologies Inc. in 3664 NIH u/mg activity in pH 6.5, 0.01 M sodium phosphate buffer, 0.2 M NaCl and 0.1% PEG-8000. r-RGD-hirudin (constructed by introducing RGD in place of ^{32}SDG^{34} in wild type 2 hirudin) was a gift from Professor Wei Mo, Molecular Medicine, Ministry of Education, Fudan University, Shanghai, China(60) and hirunorms IV and V were gifts from Prof. Pavone University of Napoli, Italy.(21;64) DCha-Pro-Nα(Me)Arg-Thr-$(Gly)_5$-^{10}Asp-Tyr-Glu-Pro-Ile-Pro-$(Glu)_2$-Ala-Cha-^{20}DGlu (Nα(Me)Arg-peptide) was a gift from Prof. Torsten Steinmetzer, Institute of Pharmaceutical Chemistry, Philipps Universität, Marburg, Germany.(65;66)

Solutions

Buffer solutions were prepared from the appropriate analytical grade salts using double distilled deionized water. All buffers were further filtered using a 0.2 μm Nylon Membrane Filter. All measurements of pH were taken with a Delta electronic pH meter.

Instruments

^{1}H NMR spectra of inhibited human α-thrombin were obtained by a Varian INOVA 600 MHz NMR instrument (Agilent Technologies, Santa Clara, CA) at the Department of Chemistry, Rutgers University, Newark, NJ and by a 600 MHz BRUKER instrument at the Center for Biomolecular Structure & Organization, Department of Chemistry & Biochemistry, University of Maryland, College Park, MD. Spectrophotometric measurements were performed with a Perkin-Elmer Lambda 6 or Lambda 35 UV-Vis Spectrophotometer connected to a PC. The temperature was monitored using a temperature

probe connected to a digital readout device. Either a Neslab RTE-4 or a Lauda 20 circulating water bath was used for temperature control.

Thrombin Activity Assay—Assays were carried out in the absence or presence of inhibitors in 1.0 mL total volume with 10 μL injection of each an appropriate solution of the substrate and thrombin. Initial rates of hydrolysis of 3-5 × 10^{-5} M (>10 K_m) S-2238 were measured by monitoring the release of 4-nitroaniline at 400 nm. Thrombin concentrations were then calculated from V_{max} values using k_{cat} = 95 ± 20 s^{-1} in pH 8.2, 0.02 M Tris buffer at 25.0 ± 0.1 °C.(51) The decline in thrombin activity was monitored for several hours after inhibition.

Trypsin Activity Assay—The inhibition of trypsin was monitored fluorometrically by the excitation of 4-methyl-umbelliferon at 365 nm and emission at 445 nm, as released from the active-site titrant MUGB in stoichiometric amount to trypsin upon reaction in pH 8.2, 0.02 M Tris buffer at 25.0 ± 0.1 °C.

Low-field ^{1}H NMR measurements—The samples were prepared by mixing 0.2-0.5 mM human α-thrombin with a slight excess of r-hirudin or its analogs, the Nα(Me)Arg-peptide and PPACK, and a > five-fold excess of D-NAPAP at pH 6.5 in 0.05 M sodium citrate buffer, or in 0.01 M phosphate buffer (pH 6.7), 0.2 M NaCl, 0.1% PEG8000. Identical concentrations and conditions were used for samples of human α-thrombin, r-hirudin and hirunorm V alone. The D_2O content was ~5-7% in general and ~ 45-59% for the isotope fractionation studies. The human α-thrombin-r-hirudin and RGD-hirudin complexes were also probed in pH 6.5, 0.020-0.040 M citrate or 0.04-0.10 M phosphate buffer which contained NaCl between 0.09 and 0.31 M concentrations. Thrombin activity was measured before and after inhibition. 97% and 98% activity loss was observed with the Nα(Me)Arg-peptide and NAPAP inhibition, respectively, and > 99% loss of activity was achieved with r-hirudin, and its mimics.

Trypsin samples were made in 1.8 mM concentration with and without ~ 3-fold excess of D-NAPAP in pH 7.00, 0.10 M phosphate buffer, 0.1% PEG-4000 and 7% D_2O. Inhibition was > 70%.

D/H fractionation factors were measured from deshielded resonances at maximal sensitivity by dividing samples identically into two, one in buffered H_2O and the other in identically buffered D_2O. Initially, the integrated peaks were referenced to a CH_2 signal on thrombin and NMR data analysis was performed in the Mestrelab Research software or using SpinWorks. This method was not always dependable, thus all quantitative measurements were replicated with an external standard.

For the D/H fractionation experiment, 270 μL of a sample was transferred in a NMR micro tube (New Era Enterprises, Vineland, NJ). A concentric capillary was inserted that contained about 60 μL of the external standard; a 1 mM CD_3CN solution of a proton sponge 1,8-bis(dimethylamino) naphthalene, which had been titrated with H_2SO_4. When using the BRUCKER spectrometer, water excitation was avoided by using a 1331 pulse sequence and a 90° pulse width of 30 μs was applied for a 512 ms acquisition time including a 2.5 s relaxation delay. One dimensional ^{1}H NMR spectra were acquired at controlled temperatures using the INOVA NMR spectrometer operating at a proton frequency of 599.7 MHz and equipped with a 5 mm triple resonance HCN probe. Typically, 2K to 16K scans of 128K complex data points over a 25 kHz spectral width were collected, preceded by a relaxation delay of 2 s. All spectra were acquired with the carrier offset placed on the water resonance which was reduced by tailored excitation, using WATERGATE(67;68) with a typical 90 deg pulse width of 7 μs. The interpulse delay of the 3-9-19 WATERGATE block

was set to 66 μs so that the spectral region of interest would be at the center of the excitation profile.

Data sets were processed on a Sun Blade 150 workstation (Sun Microsystems Inc., Palo Alto, CA) using the vnmrj software package (Agilent Technologies, Santa Clara, CA). In order to improve the signal-to-noise and the definition of the SHB NMR peak, a line broadening of 50 Hz was applied followed by baseline correction. Spectra were referenced to the sponge standard which was referenced vs DSS at 0.00 ppm.

Fractionation factors (ϕ)were calculated from the integrated signals in ~5-7% and ~45-59% D_2O buffers as follows: I = [Imax(X)] /[ϕ(1-X)+X], where X = mole fraction of H_2O; I = observed intensity and Imax is maximal intensity at X = 1.0.

The pH dependence of the resonance observed with the thrombin-r-hirudin sample was studied between pH 7.5 and 8.8 by elevating the pH of a sample, as described above, in five increments by adding aliquots of a 0.1 M or 1.0 M Na_2CO_3 solution and running the spectrum at 25 °C with the proton sponge present. Another sample was studied by decreasing the pH between 6.7 and 5.6 by adding aliquots of a 0.2 M HCl solution and recording the spectrum under identical conditions.

Results

Low-field ^{1}H NMR spectra

Low-field segments of high-resolution ^{1}H NMR spectra are exhibited in Figure 1; one obtained for a pure human α-thrombin solution, one for a pure r-hirudin solution, one for a solution of the human α-thrombin-r-hirudin complex, one for a solution of the active-site-modified human α-thrombin with PPACK and one for a solution containing PPACK-modified thrombin and r-hirudin. No signals could be observed with chemical shifts greater than 12 ppm from DSS in buffered solutions of human α-thrombin and r-hirudin or hirunorm V (not shown). In our earlier work, buffered solutions of human α-thrombin between pH 5.3 and 8.5 did not display any resonances with chemical shift greater than 12 ppm in ^{1}H NMR spectra recorded at 600 MHz.(22) A signal at 18.13 ppm is present for the covalently bound and cross-linked adduct with PPACK and one at 15.33 ppm is exhibited for the complex with r-hirudin. Addition of two equivalents of r-hirudin to the PPACK-inhibited enzyme does not cause a perceptible change in the spectrum. But addition of PPACK to the thrombin-r-hirudin complex gives a new resonance at 18.03 ppm, shifted 0.1 ppm upfield from the resonance obtained in the absence of r-hirudin. The resonances in Figure 1 are for SHBs at the active site in the case of PPACK and at a binding site with r-hirudin. Spectra identical to those shown were obtained in three repeats with PPACK-inhibited and with r-hirudin-inhibited human α-thrombin from two different sources. Both r-hirudin type 2 and 1 give the resonance. The proton exchange rate constant could be estimated from peak width at half peak height at ~ 60 Hz for the PPACK-adduct and ~ 98 Hz for the thrombin-r-hirudin complex. If there is no dipolar contribution to the line width, (28;69) the proton-exchange rate constants with solvent can be calculated to be 188 s^{-1} and 307 s^{-1} at 30 °C for the thrombin adduct with PPACK and for the r-hirudin complex, respectively. Polarization effects seemed to cause peak broadening at 5 °C. This observation is consistent with an earlier report of Frey and coworkers.(28)

Significantly, the 15.33 ppm resonance observed with the thrombin-r-hirudin complex remains unchanged in chemical shift, line width, and intensity between pH 5.6 and 8.8. This precludes the participation in a H-bond, of groups that change protonation state in this pH range.

In Figure 2 low-field spectra for complexes of thrombin with hirudin mimics and D-NAPAP are shown. The resonances for the thrombin complexes are 15.54 ppm with RGD-hirudin, 15.23 and 15.17 ppm with hirunorm IV and V, and 15.40 ppm with the Nα(Me)Arg-peptide. The thrombin complex with D-NAPAP yields a weak signal at 15.35 ppm from DSS. Although we used the racemic form of NAPAP, thrombin presents a ~1000-fold preference for the D-enantiomer. D-NAPAP was in >5-fold excess of thrombin. An analogous experiment with 1.3 mM porcine trypsin-D-NAPAP complex at pH 7.0 did not display a resonance above 15 ppm. We have examined the resonance for the thrombin-hirunorm IV complex in the temperature range 5 to 35 °C, as shown on Figure 3. The resonance shifts to lower field with decreasing temperature consistent with stronger H-bond at lower temperature. The peak broadening is probably due to polarization or to decreasing solubility and aggregation of the complex.

The resonances for the human α-thrombin-r-hirudin and RGD-hirudin complexes are insensitive to the concentration of Na^+ ions in the concentration range of 0.09-0.31 M.

For studies of equilibrium deuterium isotope effects, the r-hirudin-inhibited human α-thrombin solution was divided into two equal parts of 125 μL and equal volumes of water in one case and heavy water in the other were added to the solutions to obtain ~5-7% and 45-59% D content, respectively. This method was used consistently for solutions of thrombin inhibited with r-hirudin, hirunorms IV and V, and RGD-hirudin. The resonances obtained for complexes with r-hirudin have chemical shifts of 15.33 ± 0.05 ppm in 6.6 % D_2O and at 15.32 ppm in 58% D_2O, independent of the concentration within the 0.1-0.5 mM range (assuring that monomeric complexes are responsible for the observation). The pair of spectra for the thrombin-r-hirudin complexes are shown in Figure 4. The resonance positioned at 19.40 ± 0.05 ppm is for the proton sponge integration standard dissolved in CD_3CN.

Fractionation factors between 0.67 and 1.0 were calculated for r-hirudin-inhibited human α-thrombin from the resonances at 15.33 ppm at pH 6.5 in 0.020 M citrate buffer, 0.10 M NaCl and 25.0 and 30.0 ± 0.1°C. The fractionation factor of 1.0 for the hirunorm V-inhibited thrombin was calculated from the 15.17 ppm resonances in 0.025 M sodium citrate buffer, 0.10 M NaCl, pH 6.5 at 30. ± 0.1°C. The fractionation factor calculated at total salt concentrations above 0.30 M was 1.15 for the complexes of thrombin with r-hirudin and RGD-hirudin. The estimated precision in the integration is 20%.

Discussion

SHBs formed at the active site of thrombin

The complex of thrombin with D-NAPAP, the non-covalent active-site modifier, yielded a weak and broad signal at 15.35 pm from 16,000 scans, with line width of 125 Hz at half peak height in contrast to the narrow peaks obtained from 3-8,000 scans with the longer peptides. H-bonds between thrombin and D-NAPAP in the predominant orientations are located in the x-ray structure at the binding site, near the active site of thrombin, as is the case with PPACK.(70;71) These inhibitors bind in the canonical mode, i.e. they form an antiparallel β-sheet with the Ser^{214}-Gly^{216} segment of thrombin. Twin H-bonds are prevalent between the backbone N and O of Gly^{216} and the O and N of Gly in the P1 position of D-NAPAP (these also occur in PPACK-modified thrombin). The x-ray crystal structures suggest an opportunity for a good H-bond. The peak at 15.35 ppm probably indicates the presence of an SHB in solution. The binding of D-NAPAP to trypsin is very similar to that of thrombin,(72) which prompted us to investigate the presence of an ^1H NMR signal in the region of interest, but we found none.

Previously, resonances with chemical shifts larger than 14 ppm have been reported for many enzymes using acid/base catalysis when the catalytic base (mostly His) is protonated (at low pH) or the enzyme is bonded covalently to an appropriate active-site modifier: these observations have been interpreted to indicate the shortening of H-bridges at the active site of the enzymes.(36) These H-bridges have been referred to as SSHBs on the basis of different correlations of H-bond length and chemical shift in model compounds,(36) proton exchange rates, and fractionation factors below unity, rather than on energetic considerations.(41-46;73;74) By these criteria, we have established the presence of a SHB in the PPACK-adduct of human α-thrombin (Fig.1), an analog of the oxyanionic tetrahedral intermediate for acylation in substrate hydrolysis. As already mentioned, this SHB is almost certainly one formed between His^{57}δNH and Asp^{102}γO. The H-donor acceptor distance for this pair in thrombin has been reported to be between 2.50 and 2.65 Å in various crystal structures of inhibited thrombin at 1.8 – 2.5 Å resolution.(7;13;57-59;75) Previously, we also described a signal at 17.34 ppm occurring in anionic phosphorylated/phosphonylated adducts of thrombin, which are analogs of the tetrahedral intermediate in deacylation in substrate hydrolysis, and again form an SHB between His^{57}δNH and Asp^{102}γO.(22) The proton exchange rates in these adducts at 30 °C are low by comparison to SHBs occurring at other enzyme active sites. This observation is consistent with the character and the location of the thrombin active site in a deep canyon.(7) Deshielded ^{1}H NMR signals observed at the active site of enzymes with or without effectors result from H-bonds occurring in low dielectric environments,(44-46) often in a cluster of other H-bonds,(47) and/or due to shortening of the distance between H-donor and acceptor pairs.(40) SHBs are often ionic which has been referred to as short ionic (SI)HBs.(47)

Notably, the resonances for the two covalently modified anionic thrombin adducts are nearly identical to those observed in the corresponding analogs of tetrahedral intermediates in the double displacement mechanism of ester hydrolysis catalyzed by cholinesterases.(36-38) The greatest chemical shifts have been observed for ionic H-bonds between the protonated catalytic His and the carboxylate ion of Asp or Glu at the active site. The ^{1}H NMR resonances for SHBs occurring at the catalytic site of serine proteases, which have been modified to form oxyanionic tetrahedral adducts, are constant between pH 5 and 9 because they have elevated pK_as(28;29;33-36;39). Neutral adducts exemplified by the hemiacetal that chymotrypsin forms with N-acetyl-L-leucyl-L-phenylalanal have chemical shifts near 15 ppm.(35) His^{57} in the complex of thrombin with NAPAP is likely to be protonated at pH 6.5 and no low-field ^{1}H NMR resonance is present in native thrombin at this pH. If NAPAP binding results in sequestering or compressing the active site of thrombin, an SHB may form in the catalytic triad, but the occurrence of an intermolecular SHB at a binding site is just as possible.

The SHBs had appeared unique to the attainment of catalytic perfection, but this idea was refuted later.(41-47) Furthermore, a surprising discovery has been an ^{1}H NMR resonance at 18.0 ppm originating not from the catalytic triad in the native rhamnogalacturonan acetylesterase, but from an adjacent SHB between two Asp residues near the oxyanion hole.(76) In fact, SHBs are frequent stabilizing elements of tertiary protein structure in compressed regions or in low dielectric fields.(77) These are the features that characterize thrombin inhibition with canonical peptide inhibitors, such as NAPAP, at the P1 and P2 binding site and even more the thrombin-hirudin interface at the FRS.

SHBs in binding interactions at remote sites

The small molecular modifiers of the thrombin active site lack critical remote interactions of natural substrates at exosites so vital to the precise function of thrombin. The exosites, especially the FRS, determine the substrate selection, which is in turn regulated by Na^+ binding at an adjacent location.(78) The regulation is mediated by water channels, which

involve some short H-bridges. No ^{1}H NMR resonances with chemical shifts greater than 12 ppm have previously been reported in protein-modifier interactions occurring outside the active site of an enzyme. The binding of the hirudin family of protein/peptide inhibitors (Table 1) to α-thrombin is unique in that it is extended and includes remote binding sites, which makes the complexes erstwhile candidates for studies of the presence, origin and location of SHBs.

Hirudin is an allosteric effector of the 'fast' conformation of α-thrombin. It is a 65 residue protein produced in the salivary glands of *Hirudo medicinalis*, the common leech, in 20 varieties of close sequence homology.(79;80) Three of the most common variants contain three disulfide bonds and sulfated Tyr$^{63'}$, Tys$^{63'}$. Hirudin interacts noncovalently but tightly with α-thrombin near the active-site cleft as well as with the FRS, which contains an abundance of basic residues.(79)

The first x-ray structure (2.3 Å) of the α-thrombin-r-hirudin complex (variant 2, Lys$^{47'}$) affords a complex picture of the key interactions:(57-59;75) It displays a bound r-hirudin structure becoming more compact and forming numerous intermolecular H-bridges when interacting with thrombin in comparison to the NMR solution structure of r-hirudin, which reveals many intramolecular H-bridges within r-hirudin.(59) Yet, r-hirudin and hirunorm V alone do not yield a resonance with chemical shift greater than 12 ppm in high-resolution ^{1}H NMR spectra (Fig.1), precluding the presence of intramolecular SHBs, but that changes when they bind to α-thrombin.

Do the resonances so consistently appearing between 15.17 and 15.54 ppm derive from SHBs at different locations with canonical and noncanonical inhibitors?

While hirudin and its mimics bind near the active site region, the x-ray structure of the complex of thrombin with this family of inhibitors presents a variety of H-bonding patterns around the active site. In fact, the S1 binding site on thrombin is not used as a result of the parallel binding mode of these inhibitors, which is in stark contrast to the canonical binding of NAPAP and PPACK to thrombin.

Again, the possibility of compression of the active site and the consequent recruiting of the traditional SHB between the catalytic His^{57}δH and Asp^{102}γO, as a result of the tight binding of inhibitors to thrombin, comes to mind. However, crystal structures of thrombin with hirudin show the same geometry of the catalytic residues, a short distance (< 2.7 Å) between N and O and an angle of >150 °, as in native thrombin.(7;79) More importantly, the pH profile for the binding of hirudin to thrombin yields a pK_a of 7.1 for His^{57}, 8.4 for the N-terminal amino group of hirudin and 9.2 for the α-amino group of Ile^{16} on thrombin engaged in a salt bridge with Asp^{194}.(81) The pK_as of 7.1 and 9.2 are identical to the ones reported for the native enzyme. Yet, the 15.33 ppm resonance is independent of the ionization of the His^{57}-Asp^{102} pair and the ionization of the N-terminal amino group of hirudin between pH 5.6 and 8.8 for the r-hirudin complexes of thrombin. This seems to preclude the location of the SHB at the active site of thrombin in the complexes with r-hirudin. The N-terminal head of r-hirudin forms a parallel β-strand with thrombin (residues 214-219) making a non-substrate like interaction. The first three residues at the N-terminus, (Ile$^{1'}$-Thr$^{2'}$-Tyr$^{3'}$ variant 2), of hirudin penetrate the active site and aryl binding site where they interact with the S2 and S3 specificity site and form H-bonds to His^{57} and Ser^{214}.

The chemical shift at 18.03 ppm appears after addition of PPACK to the human α-thrombin-r-hirudin complex. PPACK probably dissociates the thrombin-hirudin complex and the spectrum may simply display two binary complexes of thrombin. The resonance for the PPACK-inhibited enzyme is 0.1 ppm upfield in the presence of r-hirudin, which may indicate increased shielding as a result of a less tightly bound PPACK in a ternary

complex(82) or a changed electrostatic environment in the active site cavity. The chemical shift at 15.33 ppm for the thrombin-r-hirudin complex remains unchanged as if the conformation of hirudin in the vicinity of the SHB remained undisturbed in the complex, but the peaks lean toward each other and broaden, which may indicate proton exchange between sites.

The central portion of hirudin is globular and is more loosely attached to α-thrombin. A C-terminal fragment of hirudin spanning residues 53-65 binds the tightest to residues 62-73 of the B-chain on α-thrombin. Strong electrostatic interactions including at least thirteen H-bonds hold this segment together, but the last five residues form a 3_{10} helical turn, which engages in hydrophobic interactions. Native hirudin with the sulfate group on $Tys^{63'}$ enhances the binding constant by ~ 15-fold over the desulfo form.(7;79;83) The intrinsic fluorescence of α-thrombin has been exploited for measurements of binding parameters, because r-hirudin binding causes key Trp residues of thrombin be buried more deeply in the interior and thus enhance its fluorescence.(84) From two studies,(15;84) it emerged that first the C-terminal segment of residues 53-65 is pre-oriented and binds rapidly to the FRS because of the complementary electrostatic forces between the two. This is followed by the fitting of the three-residue N-terminal segment, which is ~ 300 times slower than the first step.

When hirunorms are complexed to α-thrombin, the ^{1}H NMR resonance becomes a little more shielded at 15.17-15.23 ppm, than in the thrombin-r-hirudin complexes. Hirunorms(21;64;85;86) were designed to be “true hirudin mimics” by containing the functionalities that interact with the α-thrombin active site region, specifically the Ser^{214}-Gly^{216} segment, and with the FRS.(79) A three-residue segment consisting of $D\text{-}Ala^{6''}$-$\beta Ala^{7''}$ (or Gly)-$\beta Ala^{8''}$ is the spacer in place of the larger $Cys^{6'}$-$Lys^{47'}$ core in hirudin. Among five hirunorms, hirunorm IV and V are the most potent.(64) X-ray structures of α-thrombin-hirunorm IV(85) and α-thrombin-hirunorm V complexes(86) show that the hirunorms bind along the B-chain partly blocking the active-site cleft by interacting with key residues in a parallel manner. The chains stretch out of the cleft and arch over to the FRS where the C-termini interact tightly. Binding probably commences with the C-terminal end as shown for r-hirudin.(15;84) The primary sequence of hirunorms IV and V differ only at the second residue, and only slightly along the C-terminal sequence. The H-bonding potential between α-thrombin and the C-terminal region of these inhibitors is similar to that of hirudin, but not so at the active site. The hirunorms bind with ~ 4 kcal/mol less energy than does hirudin. (21;85)

r-RGD-hirudin is r-hirudin embellished with an $^{32}RGD^{34}$ (instead of SDG) sequence known to be critical for binding to the FRS of thrombin.(60) The interaction with thrombin is also enhanced at the C-terminus, where more Glu, Asp and Pro residues are present to enhance hydrophobicity. Certainly, the deshielding of the ^{1}H NMR signal by 0.21 ppm relative to r-hirudin is consistent with changes in the milieu of the key binding region at the FRS.

The ^{1}H NMR signal obtained with the complex of the Nα(Me)Arg-peptide with thrombin is essentially the same as the one for thrombin-r-hirudin complex implying that the same or similar binding elements are involved in the two cases. The Nα(Me)Arg-peptide was designed for enhanced binding affinity and storage stability by introducing methylation of the Arg in the P1 position.(65) A close analog of the C-terminal peptide of hirudin is tethered to the N-terminal segment with a poly-Gly linker in the Nα(Me)Arg-peptide, which interacts with human α-thrombin with a K_i= 37 pM.

The resonances measured between 15.17 and 15.54 ppm are consistent with donor-acceptor distances <2.70 Å, on the basis of correlations between chemical shift and H-donor acceptor

distances in small molecular crystals measured by x-ray.(36-38;40;87-89) This compares very well with the crystallographic data for the donor acceptor distance in certain H-bonds between α-thrombin and r-hirudin, RGD-hirudin and hirunorms. The exchange rates with solvent are smaller than those observed for SHBs in other enzymes,(36;88) which suggests a hydrophobic or dry environment of the SHB. In fact, contraction of the H-donor acceptor distance would lead to water exclusion.(90)

Sequence specificity of the ^{1}H NMR resonances

On the basis of the x-ray structure,(3;57;58) three regions can be identified at the α-thrombin-r-hirudin interface, where the SHB associated with 15.33 ppm signal may originate. The candidates participating from r-hirudin are, $Ile^{1'}$, $Tyr^{3'}$ $Val^{21'}$ and the $Glu^{57'}$ $Glu^{58'}$ pair, the binding epitope in fibrinogen. 1) The pH and Na^+ ion independence of the 15.33 ppm resonance negates the H-bond at the N-terminal amino group to be the origin of the chemical shift in the thrombin-r-hirudin complex. 2) Hirunorms contain a β-(2-naphthyl)alanine at the P3 site, which is an unlikely H-bonding partner to H-donors and acceptors at the active site of thrombin, yet the resonance at 15.17 ppm persists in the ^{1}H NMR spectrum. 3) Participation of $Val^{21'}$ is abrogated in the hirudin mimics yet they display the 15.17 or 15.33 ppm ^{1}H NMR resonance. 4) This leaves the most plausible site of the SHB to be, imbedded among hydrophobic residues at the C-terminus of hirudin, between $Glu^{57'}$ or $Glu^{58'}$, as H acceptors, and Arg^{75} and Arg^{77} of thrombin as H donors. In fact Arg^{75} and Arg^{77} are solvated with water, which are reported to involve H-donor-acceptor distances of 2.6-2.8 Å.(57;58) The most likely site of SHBs is the region shown in Figure 5. The pH independence between pH 5.6 and 8.8 of the 15.33 pm peak is consistent with an SHB between a carboxylate ion and guanidinium ion (Arg).

Character of proton bridges in binding

The fractionation factors for the signal at 15.17 to 15.54 ppm are near 1.0 or somewhat lower with 20% estimated error. Whereas these values are not as precise as desired, they certainly are in line with what has been found with H-bridges that resonate near 15 ppm. A D/H fractionation factor (ϕ) for a H-bridge is essentially an equilibrium constant for the exchange of H/D between a site on a protein and the protic solvent, i.e. L_2O (L=H,D). In this case, proton bridging occurs at a tight binding site. The equilibrium constant for the process can be defined as ϕ = [Binding site-D][Hsolvent]/[Binding site-H][Dsolvent], indicating the preference of the binding site for D over H in reference to the solvent, i.e. an inverse deuterium solvent isotope effect. In general, the shorter and stronger the H-bond, the smaller the value of ϕ.(36;73;91) Fractionation factors measured for H-bonds that resonate at low field are generally smaller than what we observed with these systems; for example, the 18.13 ppm signal for thrombin covalently modified by PPACK has a fractionation factor of 0.45 ± 0.04.(22)

The temperature dependence of the chemical shift for the thrombin-hirunorm-IV complex demonstrates that the SHB remains in slow-exchange with solvate and other proton donors-acceptors up to at least 35 °C.

In conclusion, using 600 MHz ^{1}H NMR on aqueous solutions of thrombin enabled us to identify SHBs in the interaction of human α-thrombin with several tight-binding inhibitors. On the basis of our earlier findings the transition state for binding of the small inhibitors doesn't show changes in the status of the H-bridges, but the stable adducts of the inhibitors with thrombin show one unique SHB at the active site. In this work we showed that strong proton bridges also enforce tight binding at external binding sites, most probably at $Glu^{57'}$-$Glu^{58'}$ in hirudin and its mimics or in the water channels. The hirudin family of inhibitors

mimic the binding propensity of fibrinogen.(79) It is therefore of substantial interest that an SHB is present when r-hirudin is bound to α-thrombin.

Acknowledgments

The generous gift of hirudin mimics is gratefully acknowledged to Professor Vincenzo Pavone, University of Napoli, Italy, Professor Wei Mo, Molecular Medicine, Ministry of Education, Fudan University, Shanghai, China, and Professor Torsten Steinmetzer, Institute of Pharmaceutical Chemistry, Philipps Universität, Marburg, Germany.

References

1. Furie B, Furie BC. The Molecular Basis of Blood Coagulation. Cell. 1988; 53:505–518. [PubMed: 3286010]
2. Davie EW, Fujikawa K, Kisiel W. The Coagulation Cascade: Initiation, Maintenance, and Regulation. Biochemistry. 1991; 30:10363–10370. [PubMed: 1931959]
3. Berliner, LJ. Thrombin: Structure and Function. Plenum Press; New York: 1992.
4. Mann KG, Lorand L. Introduction: Blood Coagulation. Methods Enzymol. 1993; 222:1–10. [PubMed: 8412787]
5. Patthy L. Modular Design of Proteases of Coagulation, Fibrinolysis, and Complement Activation: Implications for Protein Engineering and Structure-Function Studies. Methods Enzymol. 1993; 222:10–22. [PubMed: 8412789]
6. Dang QD, Vindigni A, Di Cera E. An Allosteric Switch Controls the Procoagulant and Anticoagulant Activities of Thrombin. Proc Natl Acad Sci U S A. 1995; 92:5977–5981. [PubMed: 7597064]
7. Di Cera E. Thrombin. Mol Aspects Med. 2008; 29:203–254. [PubMed: 18329094]
8. Huntington JA. How Na^+ activates thrombin--a review of the functional and structural data. J Biol Chem. 2008; 389:1025–1035.
9. Stone SR, Betz A, Hofsteenge J. Mechanistic Studies on Thrombin Catalysis. Biochemistry. 1991; 30:9841–9848. [PubMed: 1911776]
10. Vindigni A, Di Cera E. Release of Fibrinopeptides by the Slow and Fast Forms of Thrombin. Biochemistry. 1996; 35:4417–4426. [PubMed: 8605191]
11. Di Cera E, Dang QD, Ayala Y, Vindigni A. Linkage at Steady State: Allosteric Transitions of Thrombin. Methods Enzymol. 1995; 259:127–144. [PubMed: 8538450]
12. Di Cera E, Dang QD, Ayala YM. Molecular mechanisms of thrombin function. Cell Mol Life Sci. 1997; 53:701–730. [PubMed: 9368668]
13. Pineda AO, Savvides SN, Waksman G, Di Cera E. Crystal Structure of the Anticoagulant Slow Form of Thrombin. J Biol Chem. 2002; 277:40177–40180. [PubMed: 12205081]
14. Lechtenberg BC, Johnson DJD, Freund SMV, Huntington JA. NMR resonance assignments of thrombin reveal the conformational and dynamic effects of ligation. Proc Natl Acad Sci USA. 2010; 107:1–6.
15. Ayala Y, Di Cera E. Molecular Recognition by Thrombin - Role of the Slow-Fast Transition, Site-Specific Ion-Binding Energetics and Thermodynamic Mapping of Structural Components. J Mol Biol. 1994; 235:733–746. [PubMed: 8289292]
16. Johnson DJD, Adams TE, Li W, Huntington JA. Crystal structure of wild-type human thrombin in the Na^+-free state. Biochem J. 2005; 392:21–28. [PubMed: 16201969]
17. Huntington JA. Slow thrombin is zymogen-like. J Thrombosis & Heamostasis. 2009; 7(Suppl.1): 159–164.
18. Vertstraete M, Zoldhelyi P. Novel Antithrombotic Drugs in Development. Drugs. 1995; 49:856–884. [PubMed: 7641602]
19. Das J, Kimball SD. Thrombin Active Site Inhibitors. Bioorg Med Chem. 1995; 3:999–1007. [PubMed: 7582987]
20. Jetten M, Peters CAM, Visser A, Grootenhuis PDJ, van Nispen JW, Ottenheijm HCJ. Peptide-derived Transition State Analogue Inhibitors of Thrombin; Synthesis, Activity and Selectivity. Bioorg Med Chem. 1995; 3:1099–1114. [PubMed: 7582983]

21. Lombardi A, De Simone G, Galdiero S, Nastri F, Pavone V. From Natural to Synthetic Multisite Thrombin Inhibitors. Biopolymers. 1999; 51:19–39. [PubMed: 10380350]
22. Kovach IM, Kelley P, Eddy C, Jordan F, Baykal A. Proton Bridging in the Interactions of Thrombin with Small Inhibitors. Biochemistry. 2009; 48:7296–7304. [PubMed: 19530705]
23. Robillard G, Shulman RG. High Resolution Nuclear Magnetic Resonance Studies of the Active Site of Chymotrypsin II. Polarization of Histidine 57 by Substrate Analogs and Competitive Inhibitors. J Mol Biol. 1974; 86:541–558. [PubMed: 4852270]
24. Robillard G, Shulman RG. High Resolution NMR Studies of the Active Site of Chymotrypsin. I. H-bounded Protons of the “Charge-Relay” System. J Mol Biol. 1974; 86:519–540. [PubMed: 4852269]
25. Frey PA, Whitt SA, Tobin JB. A Low-Barrier Hydrogen Bond in the Catalytic Triad of Serine Proteases. Science. 1994; 264:1927–1930. [PubMed: 7661899]
26. Tobin JB, Whitt SA, Cassidy CS, Frey PA. Low-Barrier Hydrogen Bonding in Molecular Complexes Analogous to Histidine and Aspartate in the Catalytic Triad of Serine Proteases. Biochemistry. 1995; 34:6919–6924. [PubMed: 7766600]
27. Cassidy CS, Lin J, Frey PA. A New Concept for the Mechanism of Action of Chymotrypsin: The Role of the Low-Barrier Hydrogen Bond. Biochemistry. 1997; 36:4576–4584. [PubMed: 9109667]
28. Lin J, Westler WM, Cleland WW, Markley JL, Frey PA. Fractionation factors and activation energies for exchange of the low barrier hydrogen bonding proton in peptidyl trifluoromethyl ketone complexes of chymotrypsin. Proc Natl Acad Sci U S A. 1998; 95:14664–14668. [PubMed: 9843946]
29. Lin J, Cassidy CS, Frey PA. Correlations of the Basicity of His 57 with Transition State Analogue Binding, Substrate Reactivity, and the Strength of the Low-Barrier Hydrogen Bond in Chymotrypsin. Biochemistry. 1998; 37:11940–11948. [PubMed: 9718318]
30. Halkides CJ, Wu YQ, Murray CJ. A Low-Barrier Hydrogen Bond in Subtilisin: ^{1}H and ^{15}N NMR Studies with Peptidyl Trifluoromethyl Ketones. Biochemistry. 1996; 35:15941–15948. [PubMed: 8961961]
31. Ash EL, Sudmeier JL, De Fabo EC, Bachovchin WW. A Low-barrier Hydrogen Bond in the Catalytic Triad for Serine Proteases? Theory Versus Experiment. Science. 1997; 278:1128–1132. [PubMed: 9353195]
32. Kahayaoglu A, Haghjoo K, Guo F, Jordan F, Kettner C, Felfoldi F, Polgar L. Low Barrier Hydrogen Bond is Absent in the Catalytic Triads in the Ground State but is Present in a Transition-state Complex in the Prolyl Oligopeptidase Family of Serine Proteases. J Biol Chem. 1997; 272:25547–25554. [PubMed: 9325271]
33. Bao D, Huskey PW, Kettner CA, Jordan F. Hydrogen Bonding to Active-Site Histidine in Peptidyl Boronic Acid Inhibitor Complexes of Chymotrypsin and Subtilisin: Proton Magnetic Resonance Assignments and H/D Fractionation. J Am Chem Soc. 1999; 121:4684–4689.
34. Zhong S, Haghjoo K, Kettner C, Jordan F. Proton Magnetic Resonance Studies of the Active Center Histidine of Chymotrypsin Complexed to Peptideboronic Acids: Solvent Accessibility to the Nδ and ε Sites can Differentiate Slow-Binding and Rapidly Reversible Inhibitors. J Am Chem Soc. 1995; 128:7047–7055.
35. Neidhart D, Wei Y, Cassidy C, Lin J, Cleland WW, Frey PA. Correlation of Low-barrier Hydrogen Bonding and Oxyanion Binding in Transition State Analogue Complexes of Chymotrypsin. Biochemistry. 2001; 40:2439–2447. [PubMed: 11327865]
36. Mildvan AS, Massiah MA, Harris TK, Marks GT, Harrison DHT, Viragh C, Reddy PM, Kovach IM. Short Strong Hydrogen Bonds on Enzymes: NMR and Mechanistic Studies. J Mol Stucture. 2002; 215:163–175.
37. Massiah MA, Viragh C, Reddy PM, Kovach IM, Johnson J, Rosenberry TL, Mildvan AS. Short, Strong Hydrogen Bonds at the Active Site of Human Acetylcholinesterase: Proton NMR Studies. Biochemistry. 2001; 40:5682–5690. [PubMed: 11341833]
38. Viragh C, Harris TKRPM, Massiah MA, Mildvan AS, Kovach IM. NMR Evidence for a Short, Strong Hydrogen Bond at the Active Site of a Cholinesterase. Biochemistry. 2000; 39:16200–16205. [PubMed: 11123949]

39. Cleland WW, Frey PA, Gerlt JA. The Low Barrier Hydrogen Bond in Enzymatic Catalysis. J Biol Chem. 1998; 273:25529–25532. [PubMed: 9748211]
40. Vishveshwara S, Madhusudhan MS, Maziel JV Jr. Short-strong hydrogen bonds and a low barrier transition state for the proton transfer reaction in RNase A catalysis: a quantum chemical study. Biophys Chem. 2001; 89:105–117. [PubMed: 11254205]
41. Scheiner S, Kar T. The Nonexistence of Specially Stabilized Hydrogen Bonds in Enzymes. J Am Chem Soc. 1995; 117:6970–6975.
42. Perrin CL, Nielson JB. "Strong" hydrogen bonds in chemistry and biology. Annu Rev Phys Chem. 1997; 48:511–544. [PubMed: 9348662]
43. Warshel A, Papzyan A, Kollman PA. On low-barrier hydrogen bonds and enzyme catalysts. Science. 1995; 269:102–104. [PubMed: 7661987]
44. Shan SO, Loh S, Herschlag D. The Energetics of Hydrogen Bonds in Model Systems: Implications for Enzymatic Catalysis. Science. 1996; 272:97–101. [PubMed: 8600542]
45. Shan SO, Hercshlag D. The change in hydrogen bond strength accompanying charge rearrangement: Implications for enzymatic catalysis. Proc Natl Acad Sci. 1996; 93:14474–14479. [PubMed: 8962076]
46. Perrin CL. Are Short, Low-Barrier Hydrogen Bonds Unusually Strong? Acc Chem Res. 2010; 43:1550–1557. and references therein. [PubMed: 20939528]
47. Fuhrmann CN, Daugherty MD, Agard DA. Subangstrom Crystallography Reveals that Short Ionic Hydrogen Bonds, and Not a His-Asp Low-Barrier Hydrogen Bond, Stabilize the Transition State in Serine Protease Catalysis. J Am Chem Soc. 2006; 128:9086–9102. [PubMed: 16834383]
48. Schowen, RL. Structural and Energetic Aspects of Protolytic Catalysis by Enzymes: Charge-Relay Catalysis in the Function of Serine Proteases. In: Liebman, JF.; Greenberg, A., editors. Mechanistic Principles of Enzyme Activity. Vol. 9. VCH Publishers; New York: 1988. p. 119-68.
49. Schowen KB, Limbach HH, Denisov GS, Schowen RL. Hydrogen bonds and proton transfer in general-catalytic transition state stabilization in enzyme catalysis. Biochim Biophys Acta. 2000; 1458:43–62. [PubMed: 10812024]
50. Schowen, RL.; Klinman, JP.; Hynes, JT.; Limbach, HH. Hydrogen Transfer Reactions. Wiley-VCH; Weinheim, Germany: 2007.
51. Enyedy EJ, Kovach IM. Proton Inventory Studies of Thrombin-Catalyzed Reactions of Substrates with Selected P and P' Sites. J Am Chem Soc. 2004; 126:6017–6024. [PubMed: 15137766]
52. Zhang D, Kovach IM. Full and Partial Deuterium Solvent Isotope Effect Studies of α-Thrombin-catalyzed Reactions of Natural Substrates. J Am Chem Soc. 2005; 127:3760–3766. [PubMed: 15771510]
53. Alvarez, FJ.; Schowen, RL. Mechanistic Deductions from Solvent Isotope Effects. In: Buncel, E.; Lee, CC., editors. Isotopes in Organic Chemistry. Vol. 7. Elsevier; Amsterdam: 1987. p. 1-60.
54. Kresge, AJ.; More O'Ferrall, RA.; Powell, MF. Solvent Isotopes Effects, Fractionation Factors and Mechanisms of Proton Transfer Reactions. In: Buncel, E.; Lee, CC., editors. Isotopes in Organic Chemistry. Vol. 7. Elsevier; Amsterdam: 1987. p. 177-273.
55. Venkatasubban KS, Schowen RL. The Proton Inventory Technique. CRC Crit Rev Biochem. 1985; 17:1–44. [PubMed: 6094099]
56. Quinn, DM.; Sutton, LD. Theoretical Basis and Mechanistic Utility of Solvent Isotope Effects. In: Cook, PF., editor. Enzyme Mechanism from Isotope Effects. CRC Press; Boston: 1991. p. 73-126.
57. Rydel TJ, Ravichandran KG, Tulinsky A, Bode W, Huber R, Roitsch C, Fenton JW. The Structure of a Complex of Recombinant Hirudin and Human α-Thrombin. Science. 1990; 249:277–280. [PubMed: 2374926]
58. Rydel TJ, Tulinsky A, Bode W, Huber R. Refined Structure of the Hirudin-Thrombin Complex. J Mol Biol. 1991; 221:583–601. [PubMed: 1920434]
59. Grutter MG, Priestle JP, Rahuel J, Grossenbacher H, Bode W, Hofsteenge J, Stone SR. Crystal structure of the thrombin-hirudin complex - a novel mode of serine protease inhibition. EMBO J. 1990; 9:2361–2365. [PubMed: 2369893]
60. Song X, Mo W, Liu X, Zhu L, Yan X, Song H, Dai L. The NMR Solution Structure of Recombinant RGD-Hirudin. Biochem Biophys Res Commun. 2007; 360:103–108. [PubMed: 17585879]

61. Liu X, Yan X, Mo W, Song H, Dai L. Spectral Assignments and Reference Data: H NMR Assignment and Secondary Structure of Recombinant RGD-Hirudin. Magn Reson Chem. 2005; 43:956–961. [PubMed: 16103990]
62. Haruyama H, Wüthrich K. Confirmation of Recombinant Desulfatohirudin in Aqueous Solution Determined by Nuclear Magnetic Resonance. Biochemistry. 1989; 28:4301–4312. [PubMed: 2765488]
63. Folkers PJM, Clore GM, Driscoll PC, Dodt J, Köhler S, Gronenborn AM. Solution Structure of Recombinant Hirudin and Lys-47-Glu Mutant: A Nuclear Magnetic Resonance and Hybrid Distance Geomentry-Dynamical Simulated Annealing Study. Biochemistry. 1989; 28:2601–2617. [PubMed: 2567183]
64. Lombardi A, Nastri F, Morte RD, Rossi A, Rosa AD, Staiano N, Pedone C, Pavone V. Rational Design of True Hirudin Mimetics: Synthesis and Characterization of Multisite-Directed α-Thrombin Inhibitors. J Med Chem. 1996; 39:2008–2017. [PubMed: 8642559]
65. Friedrich R, Steinmetzer T, Huber R, Sturzebecher J, Bode W. The Methyl Group of N^{α}(Me)Arg-containing Peptides Disturbs the Active-site Geometry of Thrombin. Impairing Efficient Cleavage. J Mol Biol. 2002; 316:869–874. [PubMed: 11884127]
66. Rehse PH, Steinmetzer T, Li Y, Konishi Y, Cygler M. Crystal Structure of a Peptidyl Pyridinium Methyl Ketone Inhibitor with Thrombin. Biochemistry. 1995; 34:11537–11544. [PubMed: 7547884]
67. Plotto M, Saudek V, Skelenar V. Gradient-tailored excitation for single-quantum NMR spectroscopy of aqueous solutions. J Biomol NMR. 1992; 2:661–665. [PubMed: 1490109]
68. Sklenar V, Piotto M, Leppik R, Saudek V. Gradient-Tailored Water Suppresion for H1-N15 HSQC Experiments Optimized to Retain Full Sensitivity. J Magn Reson A. 1993; 102:241–245.
69. Mildvan AS, Harris TK, Abeygunawardana C. Nuclear Magnetic Resonance Methods for the Detection and Study of Low-Barrier Hydrogen Bonds on Enzymes. Methods Enzymol. 1999; 308:219–245. [PubMed: 10507007]
70. Banner DW, Hadvary P. Crystallographic Analysis at 3.0-Å Resolution of the Binding to Human Thrombin of Four Active Site-directed Inhibitors. J Biol Chem. 1991; 266:20085–20093. [PubMed: 1939071]
71. Brandstetter H, Turk D, Hoeffken HW, Grosse D, Stürzebecher J, Martin PD, Edwards BFP, Bode W. Refined 2.3 Å X-ray Crystal Structure of Bovine Thrombin Complexes Formed with the Benzamidine and Arginine-based Thrombin Inhibitors NAPAP, 4-TAPAP and MQPA. J Mol Biol. 1992; 226:1085–1099. [PubMed: 1518046]
72. Bode W, Turk D, Stürzebecher J. Geometry of binding of the benzamide- and arginine-based inhibitors N α-(2-naphthyl-sulphonyl-glycyl)-DL-p-amidinophenylalanyl-piperidine (NAPAP) and (2R,4R)-4-methyl-1-[N α-(3-methyl-1,2,3,4-tetrahydro-8-quinolinesulphonyl)-L-arginyl]-2-piperidine carboxylic acid (MQPA) to human α-thrombin. X-ray crystallographic determination of the NAPAP-trypsin complex and modeling of NAPAP-thrombin and MQPA-thrombin. Eur J Biochem. 1990; 193:175–182. [PubMed: 2226434]
73. Cleland WW, Kreevoy MM. Low Barrier Hydrogen Bonds and Enzymic Catalysis. Science. 1994; 264:1887–1890. [PubMed: 8009219]
74. Hibbert F, Elmsley J. Hydrogen Bonding and Chemical Reactivity. Adv Phys Org Chem. 1990; 26:255–379.
75. Priestle JP, Rahuel J, Rink H, Tones M, Grutter MG. Changes in interactions in complexes in hirudin derivatives and human α-thrombin due to different crystal forms. Protein Sci. 1993; 2:1630–1642. [PubMed: 8251938]
76. Langkilde A, Kristensen S, et al. Short strong hydrogen bonds in proteins: a case study of rhamnogalacturonan acetylesterase. Acta Crystallogr D-Biol Crystallogr. 2008; 64:851–863. [PubMed: 18645234]
77. Rajagopal S, Vishveshwara S. Short Hydrogen bonds in proteins. FEBS J. 2005; 272:1819–1832. [PubMed: 15819878]
78. Pineda AO, Carrell CJ, Bush LA, Prasad S, Caccia S, Chen ZW, Mathews FS, Di Cera E. Molecular Dissection of Na^{+} Binding to Thrombin. J Biol Chem. 2004; 279:31842–31853. [PubMed: 15152000]

79. Stone SR, Betz A, Parry MA, Jackman MP, Hofsteenge J. Molecular basis for the inhibition of thrombin by hirudin. Adv Exp Med Biol. 1993; 340:35–49. [PubMed: 8154342]
80. Sohn JH, Kang HA, Rao KJ, Kim CH, Choi ES, Chung BH, Rhee SK. Current status of the anticoagulant hirudin: its biotechnological production and clinical practice. Appl Microbiol Biotechnol. 2001; 57:606–613. [PubMed: 11778867]
81. Betz A, Hofsteenge J, Stone SR. pH Dependence of the Interaction of Hirudin with Thrombin. Biochemistry. 1992; 31:1168–1172. [PubMed: 1734964]
82. Stone SR, Braun PJ, Hofsteenge J. Identification of Regions of α–Thrombin Involved in its Interaction with Hirudin. Biochemistry. 1987; 26:4617–4624. [PubMed: 3663613]
83. Stone SR, Hofsteenge J. Kinetics of the Inhibition of Thrombin by Hirudin. Biochemistry. 1986; 25:4622–4628. [PubMed: 3768302]
84. Jackman MP, Parry MAA, Hofsteenge J, Stone SR. Intrinsic Fluorescence Changes and Rapid Kinetics of the Reaction of Thrombin with Hirudin. J Biol Chem. 1992; 267:15375–15383. [PubMed: 1639783]
85. Lombardi A, Simone GD, Nastri F, Galdiero S, Morte RD, Staiano N, Pedone C, Bolognesi M, Pavone V. The crystal structure of α-thrombin-hirunorm IV complex reveals a novel specificity site recognition mode. Protein Sci. 1998; 8:91–95. [PubMed: 10210187]
86. De Simone G, Lombardi A, Galdiero S, Nastri F, Della Morte R, Staiano N, Pedone C, Bolognesi M, Pavone V. Hirunorms are true hirudin mimetics. The crystal strcture of human α-thrombin-hirunorm V complex. Protein Sci. 1998; 7:243–253. [PubMed: 9521099]
87. Tolstoy PM, Smirnov SN, Shenderovich IG, Golubev NS, Denisov GS, Limbach HH. NMR studies of solid state-solvent and H/D isotope effects on hydrogen bond geometries of 1:1 complexes of collidine with carboxylic acids. J Mol Struct. 2004; 204:19–27.
88. Harris TK, Mildvan AS. High-Precision Measurement of Hydrogen Bond Lengths in Proteins by Nuclear Magnetic Resonance Methods. Proteins: Struct Funct Genet. 1999; 35:275–282. [PubMed: 10328262]
89. Fukutani A, Naito A, Tuzi S, Saitô H. Determination of principal components and their directions of ^{15}N chemical shift tensor and N-H bond lengths in simple peptides as parameters for characterization of N-H···O=C hydrogen bonds. J Mol Struct. 2001; 202:491–503.
90. Lin J, Frey PA. Strong Hydrogen Bonds in Aqueous and Aqueous-Acetone Solutions of Dicarboxylic Acids: Activation Energies for Exchange and Deuterium Fractionation Factors. J Am Chem Soc. 2000; 122:11258–11259.
91. Smirnov SN, Benedict H, Golubev NS, Denisov GS, Kreevoy MM, Schowen RL, Limbach HH. Exploring zero-point energies and hydrogen bond geometries along proton transfer pathways by low-temperature NMR. Can J Chem. 1999; 77:943–949.

Abbreviations

Cha	cyclohexyl-β-alanine
Chg	Cylohexylglycine
DMSO	dimethyl sulfoxide
DSS	4,4-dimethyl-4-silapentane-1-sulfonic acid sodium salt
MUGB	4-methylumbelliferyl 4-guanidinobenzoate hydrochloride
NAPAP	Nα-2-naphthylsulfonyl-glycyl-DL-4-amidinophenylalanyl-piperidide acetate salt
Nα(Me)Arg-peptide	DCha-Pro-Nα(Me)Arg-Thr-$(Gly)_5$-^{10}Asp-Tyr-Glu-Pro-Ile-Pro-$(Glu)_2$-Ala-Cha-^{20}DGlu
Pip	piperidyl
PPACK	Phe-Pro-Arg-Chloromethylketone

r-hirudin	recombinant hirudin type 1 or 2
r-RGD-hirudin	recombinant ^{32}SGD^{34} type 2 hirudin
S-2238	H-D-Phe-Pip-Arg-pNA
SHB	short hydrogen bond
TLC	thin layer chromatography

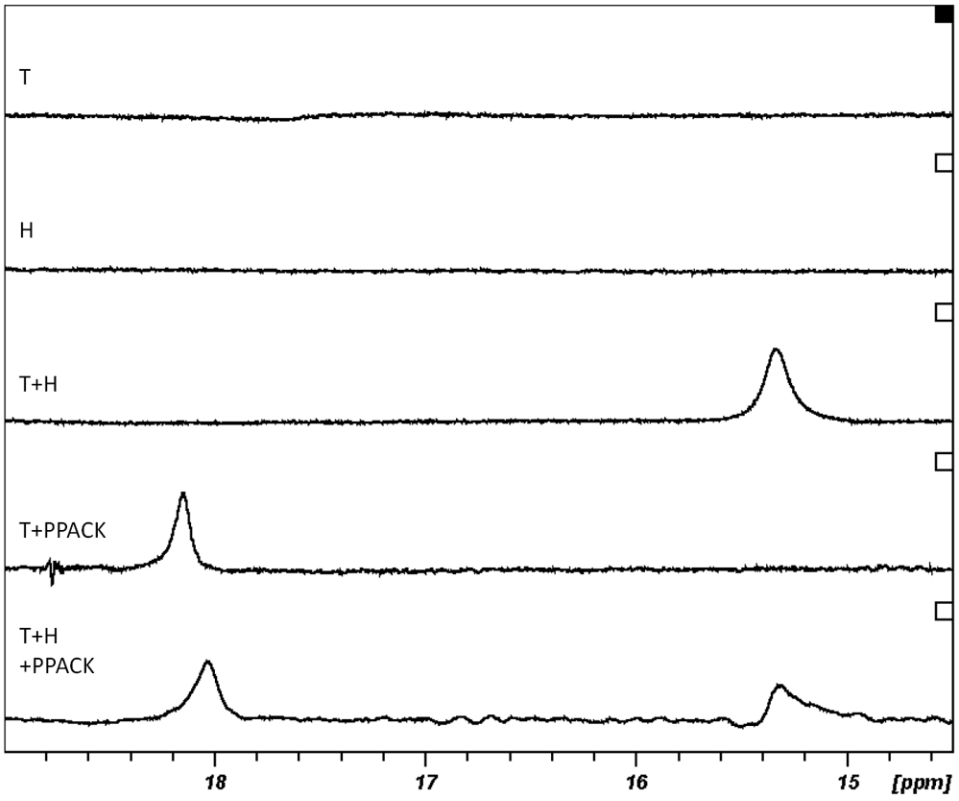

Figure 1.

Low-field sections of 3000 transients of 600 MHz ^{1}H NMR spectra of human α-thrombin and its inhibited forms at pH 6.5, 0.2 M NaCl, and 0.01% PEG800 at 30.0 ± 0.1°C and 7% D_2O: lines; T, human α-thrombin in 0.05 M citrate buffer; H, r-hirudin in 0.01 M phosphate buffer; T+H, r-hirudin-inhibited thrombin in 0.05 M citrate buffer; T+PPACK, PPACK-inhibited thrombin in 0.05 M citrate buffer; and T+H+PPACK, PPACK was added to the thrombin-r hirudin complex. The line width at half height is 60 Hz for the thrombin-PPACK adduct and 98 Hz for the thrombin-hirudin complex.

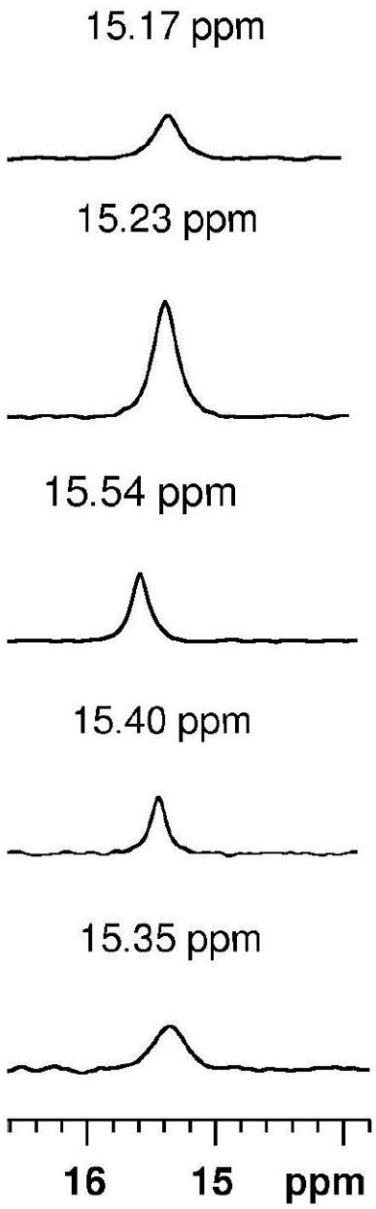

Figure 2.

Low-field region of the spectra (3-4,000 transients) obtained for complexes of human α-thrombin with hirunorm V, hirunorm IV, RGD-hirudin, Nα(Me)Arg-peptide and NAPAP from top to bottom, respectively, in pH 6.5, 0.025-0.050 M citrate buffer, 0.10-0.20 M NaCl, 0.005-0.010 % PEG-8000 at 30 °C. The corresponding peak widths at half height are 91, 82, 43, 38 and 125 Hz.

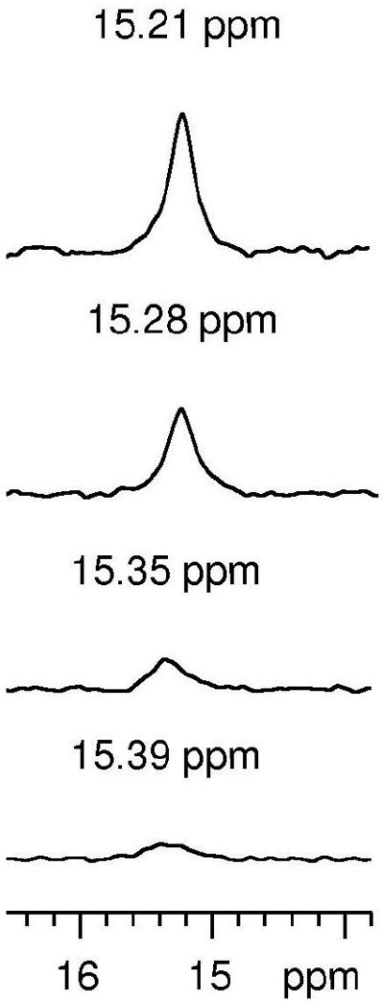

Figure 3.

Temperature dependence of the low-field resonance for the human α-thrombin-hirunorm IV complex in pH 6.5, 0.020 M citrate buffer, 0.10 M NaCl and 0.005% PEG8000. The spectra were recorded at 35, 25, 15, and 5 °C, from top to bottom.

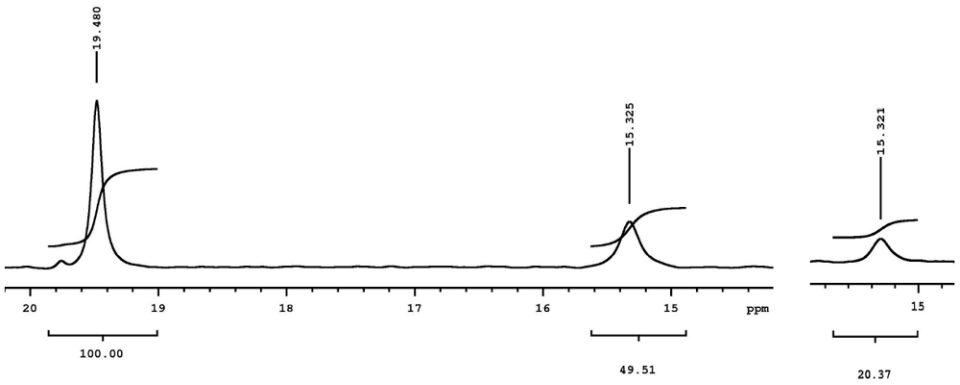

Figure 4.

Display of the integration of the resonances obtained for the proton sponge (left) and the thrombin hirudin complexes in 6.6% D_2O (middle) and in 58% D_2O (right), both buffered at pH 7.5, 0.30 M HEPES buffer, 0.30 M glycine, 0.10 M NaCl, and 0.005% PEG8000 at 25.0 ± 0.1°C.

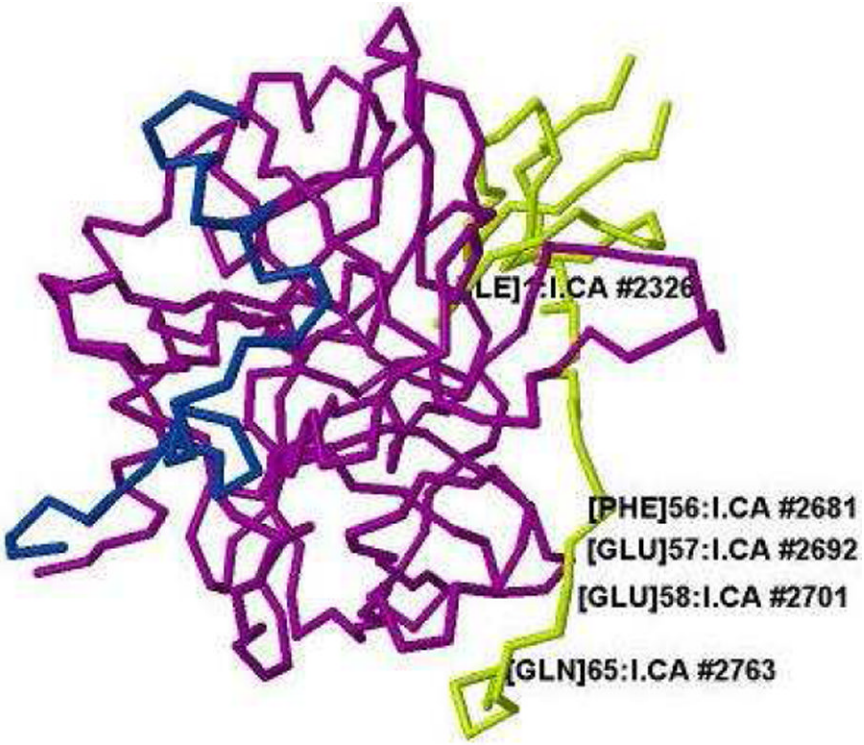

Figure 5.
The strand structures of the A chain in blue and B chain in cyan of thrombin complexed with hirudin in yellow. Ile$^{1'}$ and the most likely site of an SHB occurring in the thrombin-r-hirudin complex, residues 55 to 65 of r-hirudin, are labeled. The image is from the PDB file 4HTC(58) modeled with Jmol Version 12.0.41.

Biochemistry. Author manuscript; available in PMC 2014 April 09.

Table 1

Comparison of the amino acid sequences of r-hirudin, (57-59;75) hirunorms,(64) R-peptide(65) and NAPAP.(72)

AA	Hirudin, Var2(Var1)	Hirunorm IV	Hirunorm V	R-peptide	NAPAP
1	$Ile^{1'}$ (V)	Chg	Chg	D-Cha	2-NGly
2	$Thr^{2'}$ (V)	Arg	Val	Pro	Phe
3	$Tyr^{3'}$	2-Nal	2-Nal	N-Me-Arg	Pip
4	$Thr^{4'}$	Thr	Thr	Thr	
5	$Asp^{5'}$	Asp	Asp		
6		D-Ala	D-Ala		
7		Gly	Gly	$(Gly)_5$	
8		B-Ala	B-Ala		
9	$Pro^{48'}$	Pro	Pro		
10	$Glu^{49'}$	Glu	Glu		
11	$Ser^{50'}$	Ser	Ser		
12	$His^{51'}$	His	His		
13	$Asn^{52'}$	h-Phe	h-Phe		
14	$Asx^{53'}$	Gly	Gly		
15	$Gly^{54'}$	Gly	Gly		
16	$Asp^{55'}$	Asp	Asp	Asp	
17	$Phe^{56'}$	Tyr	Tyr	Tyr	
18	$Glu^{57'}$	Glu	Glu	Glu	
19	$Glu^{58'}$	Glu	Glu	Pro	
20	$Ile^{59'}$	Ile	Ile	Ile	
21	$Pro^{60'}$	Pro	Pro	Pro	
22	$Glu^{61'}$	Aib	Aib	Glu	
23	$Glu^{62'}$	Aib	Aib	Glu	
24	$Tyr^{63'}$	Tyr	Tyr	Ala	
25	$Leu^{64'}$	Cha	Cha	Cha	
26	$Gln^{65'}$	D-Glu	D-Glu	D-Glu	

Aib α-aminoisobutyric acid
Cha β-cyclohexyl-Ala

Chg cyclohexyl-Gly
h-Phe (+)-α-amino-4-phenylbutyric acid
2-Nal β-(2-naphtyl)-alanine
2-Ngl β-(2-naphtyl)-glycine